RESEARCH ARTICLE

Fine-Tuning Supramolecular Assemblies by Controlling Micellar Aggregates

Dipankar Ghosh, Libby J. Marshall, Giuseppe Ciccone, Wanli Liu, Adam Squires, Annela Seddon, Massimo Vassalli,* and Dave J. Adams*

Supramolecular assembly can be used to fabricate complex functional materials by organizing simple building blocks. However, it is difficult to control the hierarchical assembly across multiple length scales. The correlation of a supramolecular gel network and a pre-gelling aggregate will help to understand how a molecular-level assembly is translated into a higher order. Here, a functional dipeptide 2NapFF is used that can assemble in different micellar structures at high pH by varying the counterion. Replacing the counterions with a divalent calcium salt results in a cross-linked gel network, or an interesting analog "gel noodles." The physical properties of the gel noodles can be varied by choosing specific micellar assemblies as the pre-gel. The mechanical rigidity of the gel networks is compared by nanoindentation and tensile testing, and the pattern to the structures of the micelles observed by small-angle X-ray scattering is correlated. The supramolecular assembly can be fine-tuned by using different micelles as the pre-gel without affecting the inherent gel-state properties.

D. Ghosh, L. J. Marshall, D. J. Adams
School of Chemistry
University of Glasgow
Glasgow G12 8QQ, UK
E-mail: dave.adams@glasgow.ac.uk

G. Ciccone, M. Vassalli
Centre for the Cellular Microenvironment
University of Glasgow
Glasgow G12 8LT, UK
E-mail: massimo.vassalli@glasgow.ac.uk

W. Liu, A. Squires
Department of Chemistry
University of Bath
Bath BA2 7AY, UK

A. Seddon
School of Physics, HH Wills Physics Laboratory
University of Bristol
Tyndall Avenue, Bristol BS8 1TL, UK

1. Introduction

Supramolecular assembly is ubiquitous in nature[1,2] and inspired by this, there is a significant bioinspired theme of research.[3–5] The objectives vary greatly, from unraveling the self-assemblies of complex biomolecules and proteins[6] to arranging simple building blocks into functional materials.[7,8] The development of low molecular weight gelators (LMWGs)[9,10] has enabled the design of semi-solid supramolecular systems with tunable properties, used for diverse applications such as drug delivery,[11,12] tissue engineering,[13,14] self-healing materials,[15,16] stimuli-responsive systems,[17,18] and media for crystal growth.[19] LMWGs are self-assembled via non-bonding interactions such as hydrogen bonding, dipole–dipole, and van der Waals interactions into structures such as fibers and tubes that entangle to immobilize the solvent.[9,10] Having self-assembled LMWGs into soft materials, it is possible to chemically cross-link structures.[9] This allows the formation of robust gels with high mechanical strengths comparable to polymeric gels,[20,21] as the coordination covalent bond is a stronger interaction compared to other nonbonding interactions. The gel-state properties depend on how the gel fibers are cross-linked and further entangled to form the gel matrix. Recent advancement in supramolecular gel has enabled us to systematically design the LMWGs to some degree,[22,23] but predicting stiffness of the gel network is still difficult. LMWGs are popular due to their ability to tune gel-state properties, which is often achieved by modifying the molecular structure, varying solvent composition, or adding an additive.[24–26] However, it is still hard to achieve fine-tuning of the mechanical strength, since even a minor alteration to the molecular structures or solvent composition can result in a significant difference in gel properties. One possible solution to the issue is to pre-assemble a particular LMWG into different structures, which would further aggregate on applying suitable triggers to form a gel network.[27,28] Such primary-level assembly can be considered as pre-gelled structures, and altering these pre-gelled structures will enable us to fine-tune the supramolecular assemblies of the gels without affecting the inherent gel-state properties (**Scheme 1**).
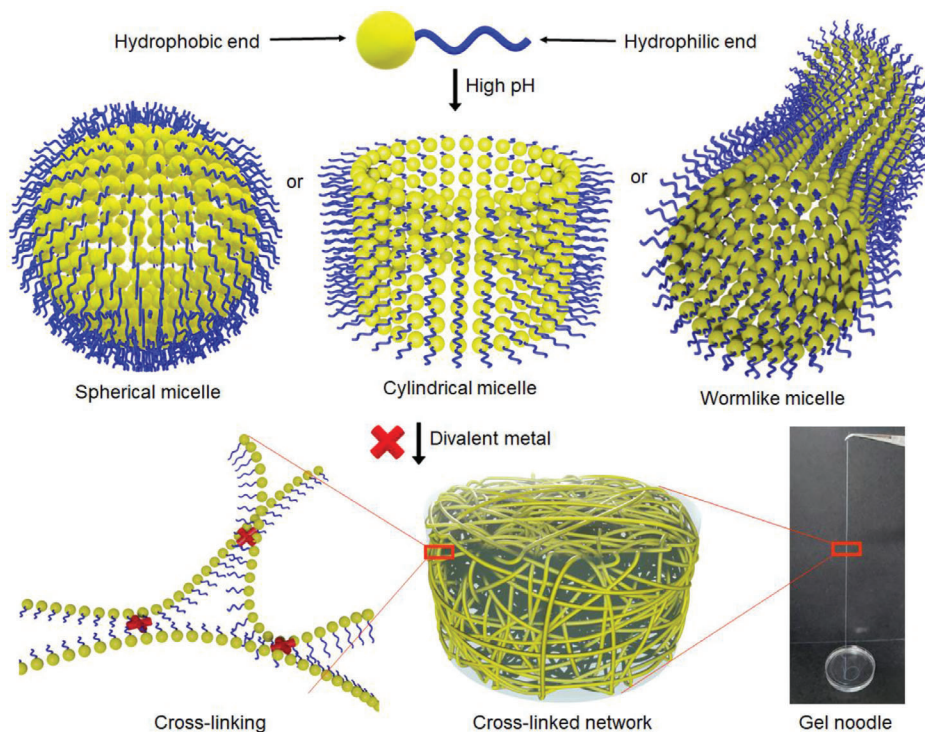
N-Functionalized dipeptides,[29] for example, 2NapFF (**Figure 1**a), form micelles at high pH.[27] The carboxylate-terminus of 2NapFF can be used to trigger gelation by reducing the pH[30]

Scheme 1. Formation of gel noodle by cross-linking of different type of micelles.

Figure 1. a) Molecular structure of 2NapFF-salts with different counterions used. b) Photograph of the 2NapFF-salts at concentrations of 20 mg mL^{-1} and pH 10.5, the counterions are indicated at the top, and the scale bar represents 2 cm. c) Viscosity diagram of the 2NapFF-salts with single counterion at 20 mg mL^{-1} and pH 10.5. d) Viscosity diagram of the same with mixed counterions.

or forming cross-linked networks by the addition of divalent cations.[31] Here, the micelles can be considered as a pre-gelled structure. 2NapFF is an ideal candidate to study the correlation between pre-gelled structure and gel-state properties since the micellar aggregation of 2NapFF has been extensively studied.[27] Also, 2NapFF is an excellent gelator forming gels with various triggers such as pH, metal salts or solvents.[30] Thus, a library of the pre-gelled structures and gel-state property of 2NapFF is

known. The correlation of these two should enable us to understand the complex gelation mechanism and will be helpful to fine-tune the gel properties.

2NapFF typically forms wormlike micelles in solution at high pH, but different structures are also possible like spherical micelles, branched micelles, etc.[27] The cylindrical micelles can also be different in terms of the length, Kuhn length, or radius. The micellar structure depends on several factors including concentration, pH, and counterion. However, the parameters like concentration and pH also significantly influence the gel-state properties. Thus, changing the micellar aggregation by altering counterions[32] is an excellent way to study the effect of different pre-gelling structures on the final gel network. Previously, our group has reported the difference in micellar arrangements of 2NapFF in the presence of various counterions, and how the properties of pH triggered gels depend on its pre-gelled structure.[33] In this work, we aim to examine the effect of varying micellar agreements on calcium-bridged cross-linked gel, also known as "gel noodles."[34–36]

2. Results and Discussion

Our group has studied 2NapFF systems at 10 mg mL^{-1} and pH 11.0 in presence of different counterions, and formation of gel network by lowering the pH to 3.6.[33] Changing the concentration of aqueous 2NapFF-salts leads to significant difference in the molecular arrangement.[27] Thus, we fixed the concentration of 2NapFF to 20 mg mL^{-1} and pH of 10.5 (within the range of ± 0.05 in all cases), and varied the counterions leading to different micellar aggregations. We used five metal ions Li$^+$, Na$^+$, K$^+$, Rb$^+$, and Cs$^+$, and two non-coordinating organic ions tetrabutylammonium (TBA) and benzyltrimethylammonium (BTMA) (Figure 1a), all added as the hydroxides to deprotonate the carboxylic acid of 2NapFF. Here, these will be referred to as 2NapFF.X, where X is the counterion used. Changing the ions from Li$^+$ to Cs$^+$ leads to an increase in the size, polarizability and softness. The Li$^+$ ion has the highest binding affinity with the carboxylate of 2NapFF and Cs$^+$ has the lowest. In contrast, the organic counterions are non-coordinating in nature, but TBA$^+$ is more hydrophobic compared to BTMA$^+$ due to the larger alkyl chains. The variation in counterion results in different micellar aggregations, and a simple way to elucidate the difference is to compare the viscosity of the solutions. The solutions prepared at 20 mg mL^{-1} and a pH of 10.5 with the organic counterions TBA$^+$ and BTMA$^+$ were visibly more viscous than the metallic counterions Li$^+$ to Cs$^+$ (Figure 1b), which is consistent with our previous reports.[27,33]

2.1. Viscosity

The 2NapFF solutions exhibited viscoelastic shear-thinning behavior[37] for all the counterions (Figure 1c). Comparison of the 2NapFF salts with a metal counterion revealed that the viscosity increased with increasing size of the counterions. 2NapFF.Li displayed the lowest viscosity among all salts and 2NapFF.Rb and 2NapFF.Cs showed highest viscosity among the metal ionic salts (Figure 1c). The small-sized Li and Na ions have higher

charge density and considered as "hard" cation, which favors binding with "hard" carboxylate moiety of 2NapFF. In contrast, the "soft" Rb and Cs ions are more labile, and this led to more viscous micellar aggregation of 2NapFF. Moving to completely non-coordinating counterions TBA and BTMA resulted in drastic increase in viscosity. 2NapFF.TBA solution was slightly more viscous than 2NapFF.BTMA, which may be attributed to the larger size and greater hydrophobicity of TBA compared to BTMA. Thus, the viscosity measurements suggest that larger size and labile nature of the counterion results in more viscous solutions.

We further studied the effect of different counterions on the micellar aggregation and viscosity by mixing two salts. For these experiments, a mixture of 2NapFF and half equivalent of two different bases were stirred overnight, followed by addition of the same mixed base at 1:1 ratio to adjust the pH to 10.5 (± 0.05). Mixing two bases could result in rearrangement of the micellar aggregation, and the resulting micelle can be different from all single-component salts. Such unique pre-gelled aggregation should enable us to construct even more fine-tuned cross-linked network. We have selected a mixed base with similar type of counterions (Li+Na), and three mixtures with unlike counterions (Li+TBA), (Na+TBA), and (Na+BTMA), in all cases as 50/50 mixtures. The viscosity of 2NapFF.(Li+Na) was similar to that of the pure 2NapFF.Li and 2NapFF.Na systems (Figure 1d), which is expected because both the single-component salts showed very similar properties. Interestingly, when a mixture of a metal-salt and an organic-salt was prepared, the mixed-salt appeared to be similar to the corresponding organic salt (Figure S1, Supporting Information). All three mixed 2NapFF.(Li+TBA), 2NapFF.(Na+TBA), and 2NapFF.(Na+BTMA)-salts showed very high viscosity, close to that of the pure 2NapFF.TBA and 2NapFF.BTMA-salts (Figure 1d). This indicates the micellar arrangement of 2NapFF.TBA and 2NapFF.BTMA-salts are dominant over the metal-salts in these systems.
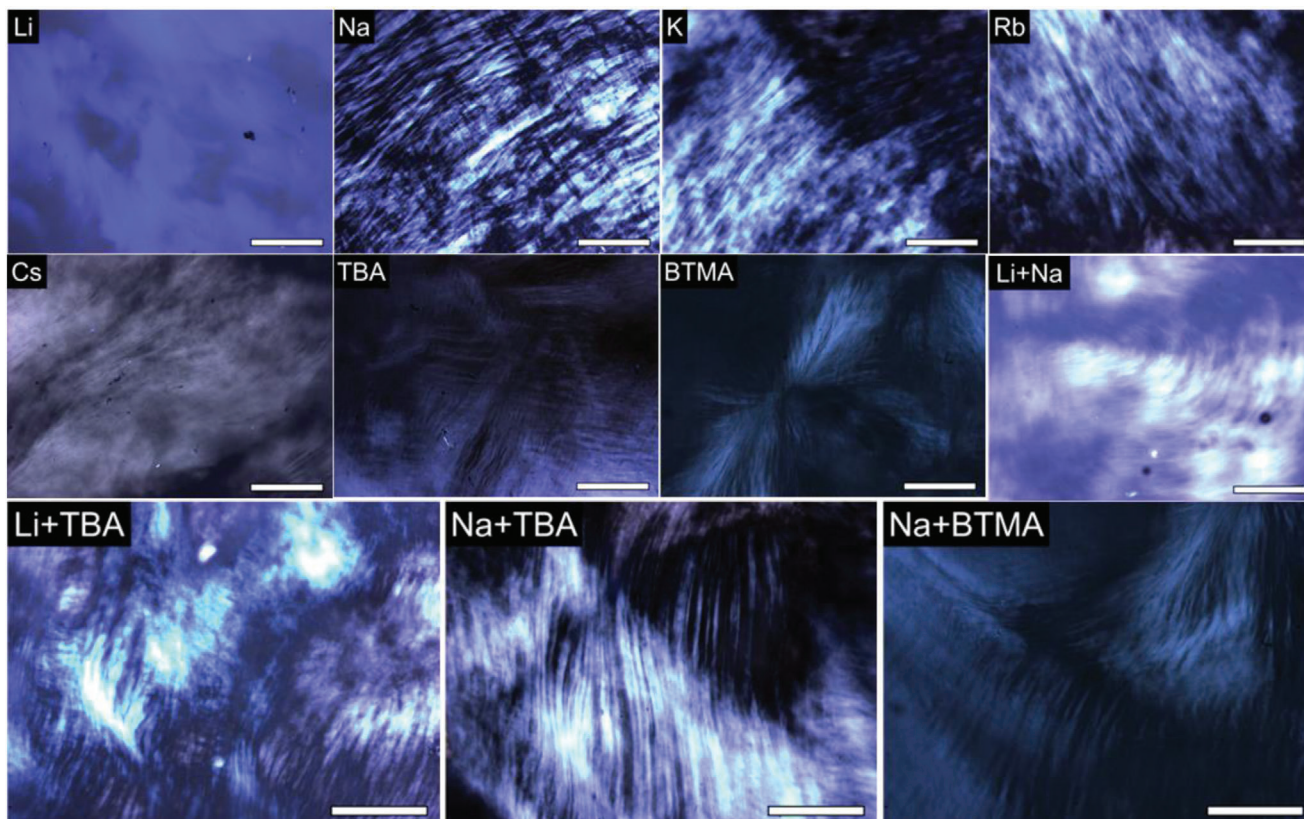
2.2. Cross-Polarized Microscopy

The micellar aggregations were examined by the cross-polarized optical microscopy[38] (CPM) images (**Figure 2**). 2NapFF solutions with all seven counterions prepared at a concentration of 20 mg mL^{-1} and pH 10.5 showed micellar aggregations in CPM images. The Li-salts displayed the highest transparency, and TBA and BTMA were found to be the most dense. The images observed for 2NapFF.(Li+Na) was comparable to pure Li- or Na-salts. The 2NapFF.(Li+TBA), 2NapFF.(Na+TBA), and 2NapFF.(Na+BTMA)-salts showed similar images to the respective pure organic counterions. Thus, the viscosity data and the microscopic images correlate well.

2.3. Small-Angle X-Ray Scattering

1D small-angle X-ray scattering (SAXS) data of the 2NapFF-salts solutions at 20 mg mL^{-1} and pH 10.5 were fitted to a flexible cylinder model (**Figure 3** and Tables S1 and S2, Supporting Information). Previous data using small-angle neutron scattering showed that the 2NapFF-Na micelles form hollow tubes,[39] but the contrast from the hollow core cannot be detected in SAXS, so

Figure 2. Cross-polarized microscopy images of the 2NapFF-salts at 20 mg mL^{-1} and pH 10.5, the counterions are indicated at the top left and scale bars represent 500 µm.
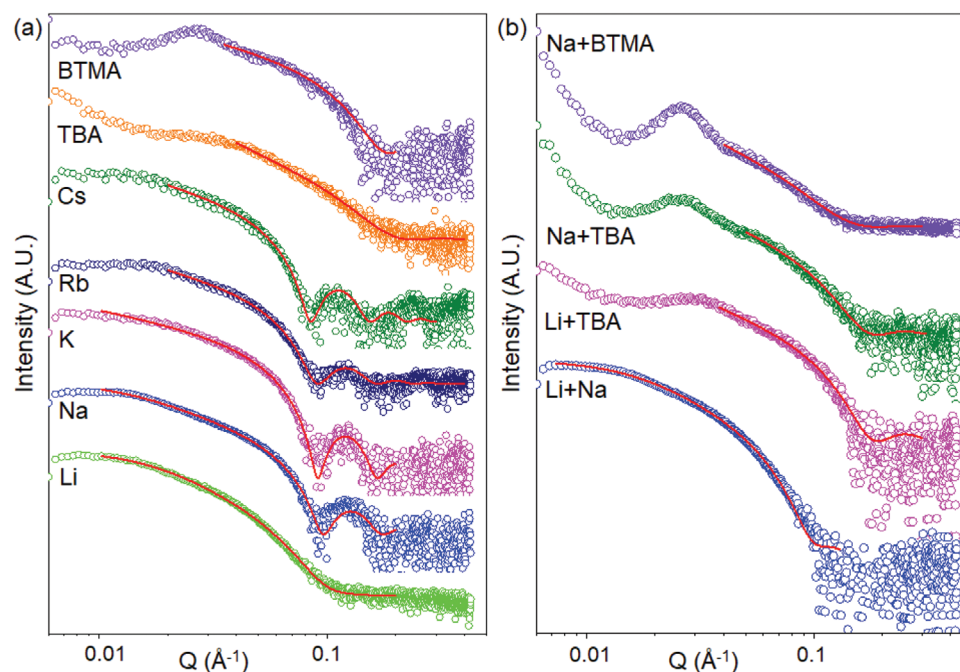
Figure 3. SAXS data of the a) 2NapFF-salts with various counterions at 20 mg mL^{-1} and pH 10.5, b) mixed 2NapFF-salt with two different counterions. The data are shown as empty circles and the fit as a red line, the counterions are labeled adjacent to the curves. The data are offset on the intensity scale for ease of discrimination and the error bars are omitted for clarity.

**ADVANCED
SCIENCE NEWS**

www.advancedsciencenews.com

[M]acro-
molecular
Materials and Engineering
Open Access

www.mame-journal.de

the flexible cylinder model is more suitable. At a concentration of 10 mg mL^{-1}, we have shown that the structures formed depend on the base used to deprotonate 2NapFF.[33]

The SAXS data obtained for each metal salt is consistent with our previous work, where the flexible cylinder model is no longer sufficient to fit 2NapFF.Li, due to the presence of helical turns and thus an elliptical cylinder model is used. Similarly, the large organic counterions TBA and BTMA lead to a far smaller radius and a Kuhn length that falls beyond the fittable range, indicating a significant stiffening of these cylinders. In the SAXS data for both 2NapFF.TBA and 2NapFF.BMTA, a structure factor peak can also be observed, indicating an interaction between individual cylinders in solution, and the onset of the semi-dilute regime of the material.[27]

In the mixed salt samples, the SAXS data showed that the 2NapFF.(Li+Na) system is still best described by an elliptical cylinder model, indicating that helicity is still present; now, however, the minor radius has decreased by 5 nm. In all cases where either Na or Li are mixed with the large organic counterions TBA or BMTA, the radius of the cylinders formed resembles that of the species formed in the organic counterion system alone, and again, a structure factor peak is present. However, unlike in the single counterion species, a measurable Kuhn length is now fitted, indicating that the samples have regained their flexibility. In all cases, the structures observed in the scattering are more similar to the structures formed by a single counterion, but with some crucial differences, such as the decreased radius of the 2NapFF.(Li+Na) sample, and the increased flexibility of the metal/organic salt cylinders. This is perhaps unsurprising, as by mixing the two salts, the concentration of each salt is decreased. This is most marked in the samples containing the metal salt and organic counterion, where the steric bulk of the organic molecule drives the formation of far thinner structures than are seen in the metal salt samples due to packing considerations; however the reduction in the Kuhn length in the 2NapFF.(Li+TBA) and 2NapFF.(Na+TBA) samples can be attributed to the reduction in the concentration of TBA. Comparing the value of the Q* structure factor peak between 2NapFF.Na and 2NapFF.(Na+TBA) shows that the mixed system has a larger correlation length than the single salt systems; the same is observed for 2NapFF.Na and 2NapFF.(Na+BMTA).

2.4. Formation of Gels

The difference in micellar arrangement of the 2NapFF molecules in the presence of various counterions was evident by viscosity, CPM images and SAXS data. Converting these micelles to a hierarchical gel network should enable us to correlate the supramolecular alignment in precursor solution and semi-solid network. We have used divalent metal salt calcium chloride to cross-link the micelle based on previous reports.[31] Cross-linking dipeptides with calcium ions results in bulk gels. When the precursor solution is extruded from a needle into a bath containing a calcium salt, highly aligned "gel noodles" are formed, with potential applications in tissue engineering, self-healing and conductive materials.[40–42] In both bulk gel and noodles, the counterions of 2NapFF are replaced with calcium; thus any difference

in the gel-network and the gel-state property will arise only from the distinct self-assembled structures in the pre-gelled form.

The bulk gels were prepared by mixing 1 mL of the CaCl$_2$ solution to 1 mL of the 20 mg mL^{-1}, pH 10.5 2NapFF-salt solutions. The molar ratio of CaCl$_2$ and 2NapFF was fixed at 1:1 by using a 40×10^{-3} M CaCl$_2$ solution. The addition of the CaCl$_2$ resulted in immediate gelation of 2NapFF in all cases (Figure S2, Supporting Information), but the texture of the gels appeared to be different. The metal-salt solutions and 2NapFF.(Li+Na) mixture formed fiber-like gels (Figure S3a, Supporting Information), whereas the organic- and mixed metal–organic salts formed granule-type gels (Figure S3b, Supporting Information).
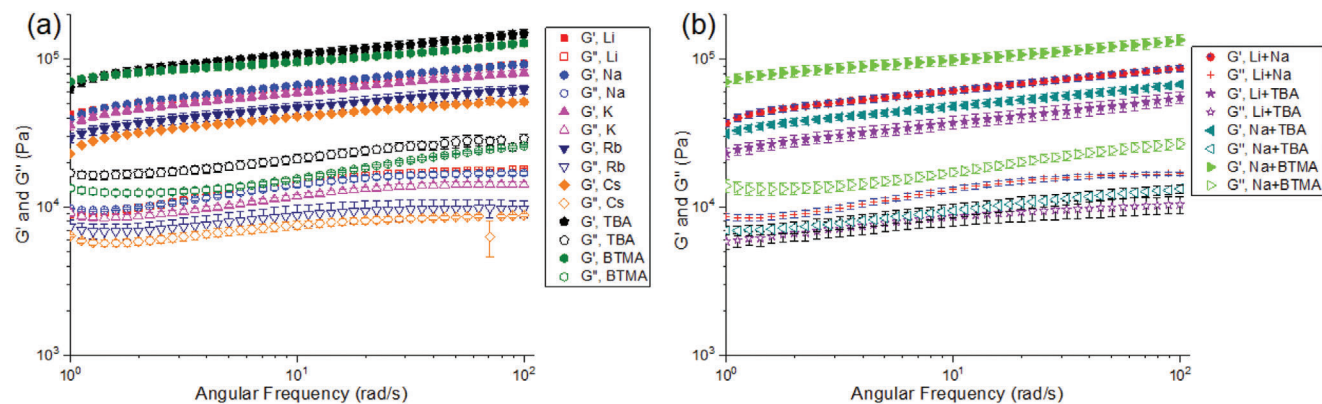
2.5. Rheology

The mechanical properties of the bulk gels were investigated by rheology.[43] The comparison of 2NapFF-metal salts + CaCl$_2$ gels revealed that the gel strength decreased with increasing size of the metal-ions (**Figure 4**a). The Li- and Na- salts displayed higher storage (G') and loss (G'') moduli and Rb- and Cs-salts showed lower G' and G'' values. Interestingly, the gels obtained from 2NapFF.TBA and BTMA showed higher G' and G'' values compared to the gels derived from all metal salts.

We also performed rheological experiments on the CaCl$_2$-gel of mixed 2NapFF salts (Figure 4b). Gels obtained using 2NapFF.(Li+Na) salt showed lower G' and G'' values compared to both 2NapFF.Li and 2NapFF.Na gels. Similarly, 2NapFF.(Li+TBA), 2NapFF.(Na+TBA) and 2NapFF.(Na+BTMA) gels with CaCl$_2$ were softer compared to the single component TBA and BTMA gels. The same trend was also seen in oscillatory strain sweep experiments (Figure S4, Supporting Information), although no significant change was observed in the crossover points of the gels.
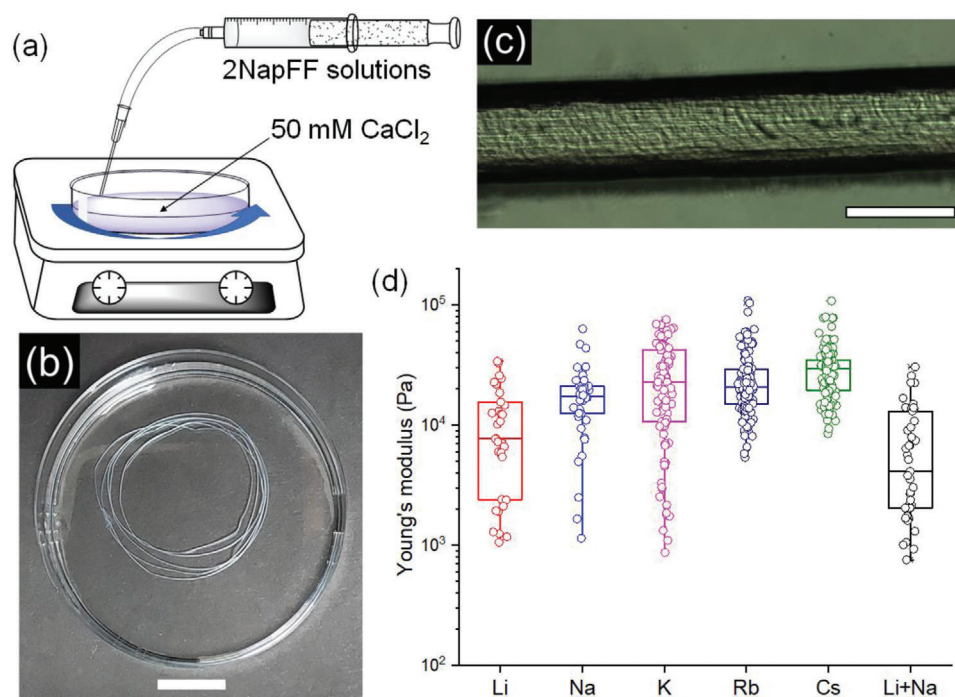
2.6. Gel Noodles

The 2NapFF solutions with different counterions were loaded in a syringe pump and extruded to a CaCl$_2$ solution rotating on a spinner (**Figure 5**a). The mixing of the pre-gel and the linker resulted in immediate gelation, and gel noodles were obtained with all seven 2NapFF salts (Figure 5b and Figure S5, Supporting Information). We used a concentration of 20 mg mL^{-1} after optimization studies. At lower concentrations, broken noodles were often formed, while at higher concentrations occlusion often occurred. When the noodles were prepared from the metal-salt solutions at 20 mg mL^{-1}, they can be usually lifted out with a tweezer. However, for 2NapFF.TBA and 2NapFF.BTMA salts, noodles were too fragile to be manipulated and measured. This is also in agreement with our previous report,[27] where noodles obtained from 2NapFF.Na were more rigid compared to the noodles obtained from 2NapFF.TBA. The noodles prepared from the organic salts were broken on application of a slight strain or shaking the petri dish. In comparison, the noodles from the metal salts were relatively robust and could resist external perturbation and deformation. Most of the noodles were also found to be stable, with the noodles from the metal salts showing no visible

ADVANCED
SCIENCE NEWS
www.advancedsciencenews.com

{M} acro-
olecular
Materials and Engineering
Open Access
www.mame-journal.de

Figure 4. Oscillatory frequency sweep experiments on the gels obtained by mixing 20 mg mL^{-1} pH 10.5 2NapFF (1 mL) and 40×10^{-3} M CaCl$_2$ (1 mL): a) comparison of various 2NapFF counterions and b) comparison of mixed-counterions.

Figure 5. a) Schematic representation of how the gel noodles are prepared, b) gel noodles obtained from 2NapFF.Li at 20 mg mL^{-1}, pH 10.5, and 50×10^{-3} M of CaCl$_2$, scale bar represents 2 cm, c) microscopic image of the 2NapFF.(Li+Na) + CaCl$_2$ gel noodle showing the aligned nanostructure in the filament, scale bar represents 500 μm, and d) statistical bar plot of nanoindentation data of gel noodles obtained from various 2NapFF salts and CaCl$_2$, the counterions of 2NapFF are shown at X-axis.

change for months (Figure S6a, Supporting Information). However, the noodles from the organic salts slowly dispersed in the solution, resulting in a thin thread and a viscous liquid (Figure S6b, Supporting Information). When the calcium chloride solution was decanted from the petri dish and deionized water was added, the noodles from organic salts dispersed within a couple of days but the noodles from metal salts were stable for at least a week.

We also prepared noodles from the mixed-2NapFF salts (Figure S7, Supporting Information). The noodles obtained from 2NapFF.(Li+Na) salt were intact when lifted from the mother liquor (similar to other single component metal-salt solutions). However, the thickness of the noodles was lower compared to both single-component 2NapFF.Li and 2NapFF.Na-salts. For mixed salts 2NapFF.(Li+TBA), 2NapFF.(Na+TBA), and 2NapFF.(Na+BTMA), noodles were formed and the morphology was similar to that of pure TBA and BTMA salts. The noodles could not be lifted from the mother liquor, were broken in pieces when shaken, and slowly dissolved in deionized water. This further indicates that mixing metal and organic salts leads to rearrangements of the micelles and the resulting micelle has similar structure to the organic salt.

**ADVANCED
SCIENCE NEWS**

www.advancedsciencenews.com

[M] macro-
molecular
Materials and Engineering
Open Access

www.mame-journal.de

The curvature and flexibility of the 1D noodles is an important structural parameter, and we quantified this by determining the persistence length.[44,45] A noodle of 10–12 cm was taken with tweezers and immersed freely in a bath of 50×10^{-3} M $CaCl_2$ solution (Figure S8, Supporting Information). The experiments could not be performed for the organic salts as it was not possible to pull up more than 1–2 cm of the noodles. The images were binarized (isodata threshold) and cleaned with morphological operators to identify the filament and extract the corresponding trajectory. The ratio of the end-to-end distance of the chains over the length was always greater than 95%. This result indicates that on the scale of about 10 cm, the noodles mostly behave as rigid rods and the persistence lengths cannot be reliably estimated. At this length scale the noodles were structurally rigid and very well aligned in 1D without any significant bending. We also imaged the noodles under CPM, which showed the aligned nanofibers in the noodles (Figure 5c and Figure S9, Supporting Information). For the metal-salts, longer nanofibers were observed in the noodle compared to the organic salts.

The formation of noodles is a fast process and the gel network is formed in a concise space. In contrast, the bulk gel was prepared in large volume (2 mL) for a period of 7 d to reach equilibrium. Thus, the entanglement of the gel network is expected to be different in the noodle and bulk gel, and the mechanical strength of the gel noodles should be different from the bulk gel. Furthermore, a 1:1 mixture of the 2NapFF-salt and $CaCl_2$ was used to prepare the gels. The bulk gels contained the excess salts/ions within the medium, which may influence the mechanical strength of the gel, as the gel-state property can be affected in both constructive or destructive ways in the presence of ions/salts.[46] We analyzed the elastic properties of the noodles to correlate the pre-gelled and gel structures, and compared the trend with the pattern observed in rheology.

2.7. Nanoindentation

We compared the relative elastic properties of the resulting noodles. Since the noodles were grown in one dimension with small diameter, bulk rheological measurements can't be performed. We evaluated the Young's modulus (E) of the noodles by nanoindentation,[47] which allows to quantify the local mechanical properties at micron length scales.[34,35,48] The noodles were placed along the X-direction on the nanoindenter, and a matrix of 25 indentions was recorded for each noodle (see experimental section). The noodles from 2NapFF.TBA and 2NapFF.BTMA salts were not characterized due to the fragile nature and dispersion in deionized water medium used in the experiments. For the same reason, noodles from the mixed salts containing TBA and BTMA were also not analyzed.

Since nanoindentation measures local mechanical properties at the micrometer length scale, the data are associated with large error bars. We have collected the matrix of 25 indentations on three different noodles and two regions of each noodle (total six matrix scans). The average E and associated standard deviation is shown in Table S3 (Supporting Information). Among all the noodles prepared from 2NapFF-metal salts, the Cs-salt displayed the highest E (Figure 5d). This implies that the micellar form of 2NapFF.Cs is cross-linked with $CaCl_2$ to produce the stiffest net-
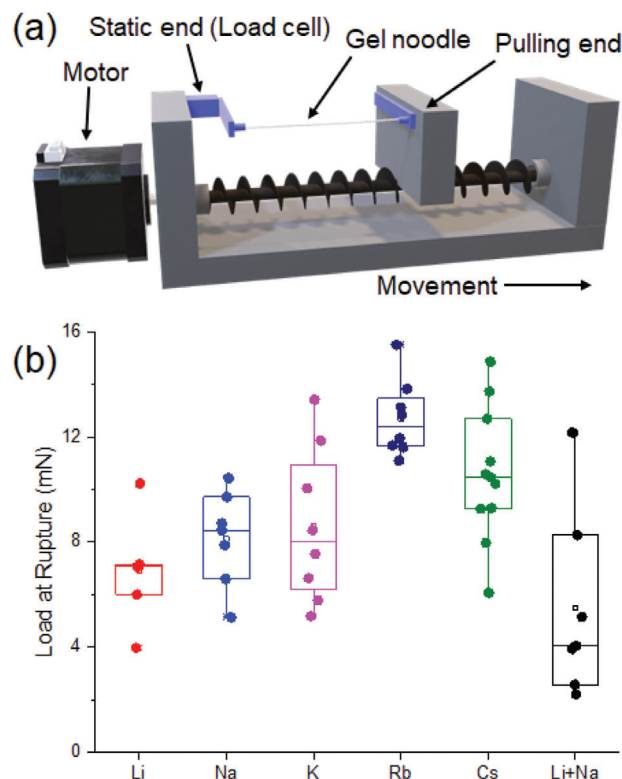
Figure 6. a) Experimental setup for the tensile testing experiments, b) statistical bar plot of the force required to rupture gel noodles obtained from various 2NapFF salts and $CaCl_2$, the counterions of 2NapFF are shown at X-axis.

work. Thus, a reverse trend was observed in rheology and nanoindentation experiments. On the other hand, Young's modulus of the noodles from the mixed 2NapFF.(Li+Na) salt was lower than both individual 2NapFF.Li and 2NapFF.Na salts. Clearly, using mixed 2NapFF-salts reduced the mechanical strength in both noodles and bulk gels.

2.8. Tensile Testing Experiments

The local mechanical properties of the gel noodles measured by nanoindentation were complemented by analyzing the axial stiffness of the noodles (i.e., along their length) by performing tensile testing experiments using a custom-built 3D printed tensile testing apparatus (**Figure 6**a). Each noodle was placed along the axis of movement and stretched at a constant speed of 25 mm min^{-1} until broken, and the forces required to rupture the noodles were compared (Figure 6b and Table S4, Supporting Information). The graph shows that the noodles from small-sized Li ion have lowest ultimate tensile strength among all single-component noodles, i.e., it requires lowest force applied to break them. The noodles from Na and K-salts exhibited slightly higher ultimate tensile strength, and larger-sized Rb and Cs-ions produced distinctly stiffer noodles. The results clearly showed that 2NapFF.Rb and Cs-noodles are more rigid along the overall length. In case of the mixed 2NapFF.(Li+Na) noodle, the ultimate tensile strength was even lower compared to both Li- and Na-noodles. This is

www.advancedsciencenews.com

{M}acro-molecular
Materials and Engineering
Open Access
www.mame-journal.de

evident that mixing two 2NapFF-salts weakens the cross-linked network across all length scales. The results corroborated well with the nanoindentation experiments and support both trends of decreasing mechanical strengths with small-sized cations and mixed counterions.

The chemical composition of the noodles was analyzed by energy-dispersive X-ray spectroscopy (EDS).[49] The characteristic K_α of the metals such as K, Rb, and Cs was not observed in the energy spectra of the corresponding noodles (Table S5, Supporting Information). This confirms that these counterions were neither chemically bonded to 2NapFF in the supramolecular chain, nor trapped in the gel network. The absence of the counterions ensures that any difference in the mechanical property of the noodles arises from the different arrangements of the pre-gelled state.

3. Conclusion

The micellar aggregation of the *N*-functionalized dipeptide 2NapFF was varied by changing the counterions at pH 10.5 and a concentration of 20 mg mL^{-1}. The group-I metals Li to Cs, organic TBA and BTMA, and four mixed ions were used in the study. The 2NapFF solutions with all the counterions formed flexible cylindrical micelles, but with increasing size of the counterions, the cylinders became more rigid as higher Kuhn lengths were observed in 1D SAXS. The different micellar aggregates were cross-linked by divalent Ca^{2+} salt to fabricate hierarchical gel networks, and controlled extrusion of the pre-gelling solution to a Ca^{2+} bath resulted in highly aligned 1D "gel noodles." The physical properties of both the bulk gels and gel noodles varied depending upon the counterions of 2NapFF solutions. The mechanical strength of the bulk gels was analyzed by rheology, which suggested that the gels from the organic salts are stiffer. However, the local mechanical strength of the noodles evaluated by nanoindentation and the overall rigidity along the 1D filaments measured in the tensile testing experiments showed that the 2NapFF solution with soft metal ions yielded stiffer noodles. The noodles resulting from the organic salts were significantly fragile. Thus, this work demonstrated that the variation of micellar arrangement can be translated to the hierarchical networks to fine-tune the gel-state properties.

4. Experimental Section

All chemicals were purchased from Sigma-Aldrich or Fluorochem Ltd. and used as supplied. Deionized water was used in all experiments. 2NapFF was synthesized following previously reported procedures.[50] The 2NapFF solutions were prepared by stirring a mixture of 400 mg (0.806 mmol) of 2NapFF, 11.94 mL of deionized water, and 8.06 mL of 0.1 M corresponding bases (LiOH to BTMAOH). The mixture was stirred overnight (≈20 h) at room temperature (≈20 °C) with a 25 × 8 mm stirrer bar in a 50 mL centrifuge tube at 1000 RPM. The pH was adjusted to 10.5 ± 0.05 using 1.0 M of the identical base. 2NapFF solutions with mixed ions were prepared by stirring 400 mg (0.806 mmol) of 2NapFF, 11.94 mL of deionized water, and 4.03 mL each of the bases (0.1 M solutions). Then the pH was adjusted with a 1:1 mixture of the two bases (1.0 M each).

Viscosity Measurement: The viscosity measurements were performed in Anton Paar Physica MCR101 rheometer using a 50 mm cone geometry (CP50). The gap between the geometry and the plate was set to 0.1 mm and temperature was kept at 25 °C. ≈1 mL of the samples was poured onto the plate to avoid any shearing caused by pipetting the solutions. All viscosity measurements were carried out in triplicates, and the mean values were plotted with the appropriate error bars.

Cross-Polarized Microscopy: A drop of the 2NapFF salt solutions was placed on a glass slide, and the microscopic images were taken on a Nikon Eclipse LV100 microscope at 5× magnification. The lights were calibrated first and then images were collected under polarized light. ImageJ software was used to insert scale bars into the images.

SAXS: Appropriate amount of different 2NapFF samples was transferred into borosilicate capillaries (BQCT 1.5 mm, Capillary Tue Supplies Ltd.), which was subsequently sealed with heat-shrinkers using a heat gun. The prepared samples were mounted horizontally onto the capillary sample rack inside a SAXS Point 2.0 (Anton Paar) for data collection. The 2D SAXS patterns were obtained from a Dectris Eiger detector using Cu source ($K_\alpha = 1.54$ Å) at a sample-to-detector distance of 576 mm, and acquisition time was 10 min for each sample. Data reduction of 2D to 1D radial profiles was performed via azimuthal integration from the Anton Paar SAXSanalysis software.

Rheology: Oscillatory frequency and strain sweep measurements were carried out in Anton Paar Physica MCR301 and MCR101 rheometers, respectively. 1 mL of 2NapFF (20 mg mL^{-1}, 0.04 mmol, at pH 10.5) salt solution was taken in a 7 mL sterilin vial, and 1 mL of 40×10^{-3} M CaCl$_2$ (0.04 mmol, 1:1 ratio) was added to it. The mixture was shaken for ≈10 s to ensure homogenous mixing, and left undisturbed for 7 d to reach equilibrium. The vial was placed on the rheometer and measurements were performed using a rotating vane geometry at gap distance of 1.8 mm between the geometry and the bottom of the sample vial. Frequency sweeps were performed at 25 °C under a strain of 0.05%. Strain sweeps were performed at 25 °C and angular frequency of 10 rad s^{-1}. The measurements were carried out in triplicate (frequency sweeps) or duplicate (strain sweep) and values were averaged. Error bars represent the standard deviation between the replicates.

Preparation of Gel Noodles: About 20 mL of 50×10^{-3} M CaCl$_2$ was placed on a petri dish (diameter 90 mm) and it was rotated on a spincoater at 100 rpm. The 2NapFF solution was extruded from Alaris Carefusion syringe pump, with a 10 mL syringe and 21-gauge needle at a flow rate of 100 mL h^{-1}.

Nanoindentation: Nanoindentation measurements were performed using a Chiaro nanoindentation device following the standardized protocol.[47] A cantilever holding a spherical tip of radius (R) 2.5 µm was used, and the stiffness (k) of the probe was 0.22 N m^{-1}. The nanoindenter was mounted on top of an inverted Zeiss Axiovert 200 M microscope. About 3 cm of a gel noodle was cut with a scissor and placed in a glass petri dish. A metal washer was kept on the top of the noodle to prevent movement. Deionized water was added to immerse the noodle and prevent drying. The petri dish was placed on the microscope stage, keeping the noodle along the *x*-direction. At least two matrix scans were performed on each noodle, and each matrix scan consisted of 25 indentations. The spacing between subsequent indentations was 6 µm. For data analysis, forward segment of the collected force–displacement (*F*–*z*) curves were analyzed using a custom open-source software.[47] The contact point was identified by a thresholding algorithm[47] to convert *F*–*z* curves into force–indentation (*F*–δ) curves. The *F*–δ curves were fitted with the Hertz model up to a maximum indentation of $\delta = 0.1R$ to quantify the elastic properties of the gels.

Tensile Testing Experiments: The axial stiffness of the noodles (i.e., along their length) was measured by performing tensile testing experiments using a custom-built 3D printed tensile testing apparatus (Figure 6a). The tensile tester was adapted from a previously published open-source stretcher/tensile tester.[51,52] The design was modified by including a 0.2 N load cell (Strain Measurement Devices, UK) and custom grips. Since noodles were too soft to be gripped, magnets were used to snap two screws in place (one connected to the load cell, and one connected to the moving part of the tensile tester). The two ends of the noodles were then wrapped around the two screws. Each noodle was stretched along its length at a speed to 25 mm min^{-1} until fracture. Both force and displacement were recorded during the experiment. A polynomial function was first fitted to the initial portion of the data (the portion where the noodle is get-

ting into tension but not being stretched), and the fit was used to detrend the raw data to create a fictitious flat baseline. This property was used to discern the portions of the curve where the noodle was getting into tension, and where the noodle was actually being stretched. Following this, the detrended data was used to find the point where the noodle starts being consistently stretched. Then, this point was subtracted from the data, and the maximum force was used to quantify the strength of the noodles.

EDS: The gel noodles were lifted from mother liquor and dipped in deionized water. It was filtered and dried in a vacuum oven at 60 °C for overnight. The EDS was performed in a Philips XL series scanning electron microscope at 20 kV.

Supporting Information

Acknowledgements

Conflict of Interest

The authors declare no conflict of interest.

Data Availability Statement

The data that support the findings of this study are available in the supplementary material of this article.

Keywords

[1] P. Ball, *The Self-Made Tapestry: Pattern Formation in Nature*, Oxford University Press, Oxford **2001**.
[2] D. Philp, J. F. Stoddart, *Angew. Chem., Int. Ed.* **1996**, *35*, 1154.
[3] J. M. Lehn, *Supramolecular Chemistry: Concepts and Perspectives*, Wiley-VCH, Weinheim, Germany **1995**.
[4] J. L. Atwood, J. M. Lehn, *Comprehensive Supramolecular Chemistry*, Pergamon, Oxford **1996**.
[5] P. W. J. M. Frederix, I. Patmanidis, S. J. Marrink, *Chem. Soc. Rev.* **2018**, *47*, 3470.
[6] D. A. Uhlenheuer, K. Petkau, L. Brunsveld, *Chem. Soc. Rev.* **2010**, *39*, 2817.
[7] S. Zhang, *Nat. Biotechnol.* **2003**, *21*, 1171.
[8] A. Levin, T. A. Hakala, L. Schnaider, G. J. L. Bernardes, E. Gazit, T. P. J. Knowles, *Nat. Rev. Chem.* **2020**, *4*, 615.
[9] E. R. Draper, D. J. Adams, *Chem* **2017**, *3*, 390.
[10] P. R. A. Chivers, D. K. Smith, *Nat. Rev. Mater.* **2019**, *4*, 463.
[11] K. J. Skilling, F. Citossi, T. D. Bradshaw, M. Ashford, B. Kellam, M. Marlow, *Soft Matter* **2014**, *10*, 237.
[12] C. C. Piras, A. K. Patterson, D. K. Smith, *Chem. - Eur. J.* **2021**, *27*, 13203.
[13] Y. Zhao, S. Song, X. Ren, J. Zhang, Q. Lin, Y. Zhao, *Chem. Rev.* **2022**, *122*, 5604.
[14] X. Wang, C. Feng, *WIREs Nanomed. Nanobiotechnol.* **2023**, *15*, e1847.
[15] X. Yu, L. Chen, M. Zhang, T. Yi, *Chem. Soc. Rev.* **2014**, *43*, 5346.
[16] A. Bayón-Fernández, A. Méndez-Ardoy, C. Alvarez-Lorenzo, J. R. Granja, J. Montenegro, *J. Mater. Chem. B* **2023**, *11*, 606.
[17] D. Díaz Díaz, D. Kühbeck, R. J. Koopmans, *Chem. Soc. Rev.* **2011**, *40*, 427.
[18] C. D. Jones, J. W. Steed, *Chem. Soc. Rev.* **2016**, *45*, 6546.
[19] D. K. Kumar, J. W. Steed, *Chem. Soc. Rev.* **2014**, *43*, 2080.
[20] X. Li, H. Wang, D. Li, S. Long, G. Zhang, Z. Wu, *ACS Appl. Mater. Interfaces* **2018**, *10*, 31198.
[21] J. Yang, F. Xu, C.-R. Han, *Biomacromolecules* **2017**, *18*, 1019.
[22] P. W. J. M. Frederix, G. G. Scott, Y. M. Abul-Haija, D. Kalafatovic, C. G. Pappas, N. Javid, N. T. Hunt, R. V. Ulijn, T. Tuttle, *Nat. Chem.* **2015**, *7*, 30.
[23] R. Batra, T. D. Loeffler, H. Chan, S. Srinivasan, H. Cui, I. V. Korendovych, V. Nanda, L. C. Palmer, L. A. Solomon, H. C. Fry, S. K. R. S. Sankaranarayanan, *Nat. Chem.* **2022**, *14*, 1427.
[24] D. Ghosh, R. Bjornsson, K. K. Damodaran, *Gels* **2020**, *6*, 41.
[25] J. Raeburn, C. Mendoza-Cuenca, B. N. Cattoz, M. A. Little, A. E. Terry, A. Z. Cardoso, P. C. Griffiths, D. J. Adams, *Soft Matter* **2015**, *11*, 927.
[26] L. E. Buerkle, S. J. Rowan, *Chem. Soc. Rev.* **2012**, *41*, 6089.
[27] L. Thomson, D. Mcdowall, L. Marshall, O. Marshall, H. Ng, W. J. A. Homer, D. Ghosh, W. Liu, A. M. Squires, E. Theodosiou, P. D. Topham, L. C. Serpell, R. J. Poole, A. Seddon, D. J. Adams, *ACS Nano* **2022**, *16*, 20497.
[28] E. R. Draper, H. Su, C. Brasnett, R. J. Poole, S. Rogers, H. Cui, A. Seddon, D. J. Adams, *Angew. Chem., Int. Ed.* **2017**, *56*, 10467.
[29] S. Fleming, R. V. Ulijn, *Chem. Soc. Rev.* **2014**, *43*, 8150.
[30] C. Colquhoun, E. R. Draper, R. Schweins, M. Marcello, D. Vadukul, L. C. Serpell, D. J. Adams, *Soft Matter* **2017**, *13*, 1914.
[31] L. Chen, G. Pont, K. Morris, G. Lotze, A. Squires, L. C. Serpell, D. J. Adams, *Chem. Commun.* **2011**, *47*, 12071.
[32] M. A. Ramin, K. R. Sindhu, A. Appavoo, K. Oumzil, M. W. Grinstaff, O. Chassande, P. Barthélémy, *Adv. Mater.* **2017**, *29*, 1605227.
[33] K. Mcaulay, P. A. Ucha, H. Wang, A. M. Fuentes-Caparrós, L. Thomson, O. Maklad, N. Khunti, N. Cowieson, M. Wallace, H. Cui, R. J. Poole, A. Seddon, D. J. Adams, *Chem. Commun.* **2020**, *56*, 4094.
[34] D. Mcdowall, M. Walker, M. Vassalli, M. Cantini, N. Khunti, C. J. C. Edwards-Gayle, N. Cowieson, D. J. Adams, *Chem. Commun.* **2021**, *57*, 8782.
[35] L. J. Marshall, M. Wallace, N. Mahmoudi, G. Ciccone, C. Wilson, M. Vassalli, D. J. Adams, *Adv. Mater.* **2023**, *35*, 2211277.
[36] S. Zhang, M. A. Greenfield, A. Mata, L. C. Palmer, R. Bitton, J. R. Mantei, C. Aparicio, M. O. de la Cruz, S. I. Stupp, *Nat. Mater.* **2010**, *9*, 594.
[37] J.-F. Berret, in *Molecular Gels: Materials with Self-Assembled Fibrillar Networks* (Eds: P. T. Richard, G. Weiss), Springer, Berlin **2006**, Ch. 19.
[38] J. R. Bellare, H. T. Davis, W. G. Miller, L. E. Scriven, *J. Colloid Interface Sci.* **1990**, *136*, 305.
[39] E. R. Draper, B. Dietrich, K. Mcaulay, C. Brasnett, H. Abdizadeh, I. Patmanidis, S. J. Marrink, H. Su, H. Cui, R. Schweins, A. Seddon, D. J. Adams, *Matter* **2020**, *2*, 764.
[40] C. M. Rubert Pérez, N. Stephanopoulos, S. Sur, S. S. Lee, C. Newcomb, S. I. Stupp, *Ann. Biomed. Eng.* **2015**, *43*, 501.
[41] S. R. Diegelmann, N. Hartman, N. Markovic, J. D. Tovar, *J. Am. Chem. Soc.* **2012**, *134*, 2028.
[42] J. López-Andarias, M. J. Rodriguez, C. Atienza, J. L. López, T. Mikie, S. Casado, S. Seki, J. L. Carrascosa, N. Martín, *J. Am. Chem. Soc.* **2015**, *137*, 893.

[43] A. Dawn, H. Kumari, *Chem. - Eur. J.* **2018**, *24*, 762.

[44] X. Li, W. Lehman, S. Fischer, *J. Struct. Biol.* **2010**, *170*, 313.

[45] M. Schneider, A. Al-Shaer, N. R. Forde, *Biophys. J.* **2021**, *120*, 2599.

[46] S. S. Jayabhavan, D. Ghosh, K. K. Damodaran, *Molecules* **2021**, *26*, 6420.

[47] G. Ciccone, M. Azevedo Gonzalez Oliva, N. Antonovaite, I. Lüchtefeld, M. Salmeron-Sanchez, M. Vassalli, *J. Visualized Exp.* **2022**, *179*, e63401.

[48] M. L. Oyen, *Curr. Opin. Solid State Mater. Sci.* **2015**, *19*, 317.

[49] B. R. Jany, A. Janas, F. Krok, *Nano Lett.* **2017**, *17*, 6520.

[50] L. Chen, K. Morris, A. Laybourn, D. Elias, M. R. Hicks, A. Rodger, L. Serpell, D. J. Adams, *Langmuir* **2010**, *26*, 5232.

[51] Y. Wang, R. Singer, X. Liu, S. J. Inman, Q. Cao, Q. Zhou, A. Noble, L. Li, A. V. Arizpe Tafoya, M. Babi, K. Ask, M. R. Kolb, S. Ramsay, F. Geng, B. Zhang, Y. Shargall, J. M. Moran-Mirabal, M. Dabaghi, J. A. Hirota, *Front. Bioeng. Biotechnol.* **2022**, *10*, 959335.

[52] X. C. Liu, *M.Sc. Thesis*, University of Toronto (Canada) **2021**.

2300082 (10 of 10)